

A VISCOELASTIC-VISCOPLASTIC-DAMAGE CONSTITUTIVE MODEL BASED ON A LARGE STRAIN HYPERELASTIC FORMULATION FOR AMORPHOUS GLASSY POLYMERS

V.-D. Nguyen¹, X. Morelle², F. Lani², T. Pardoën², C. Bailly³ and L. Noels¹

¹Computational & Multiscale Mechanical of Materials (CM3),
Department of Aerospace and Mechanical Engineering (LTAS), University of Liège
Quartier POLYTECH 1, allée de la Découverte 9, 4000 Liège, Belgium
Email: {vandung.nguyen, l.noels}@ulg.ac.be, web page: <http://www.ltas-cm3.ulg.ac.be/>

²Material and Process Engineering (IMAP),
Institute of Mechanics, Materials and Civil Engineering (iMMC), University of Louvain
Place Sainte Barbe 2 bte L5.02.02 à 1348 Louvain-la-Neuve, Belgium
Email: {xavier.morelle, frederic.lani, thomas.pardoën}@uclouvain.be,
web page: <http://www.uclouvain.be/en-imap>

³Bio and Soft Matter (BSMA),
Institute of Condensed Matter and Nanosciences (IMCN), University of Louvain
Croix du Sud 1 bte L7.04.02 à 1348 Louvain-la-Neuve, Belgium
Email: christian.bailly@uclouvain.be, web page: <http://www.uclouvain.be/en-bsma>

Keywords: Hyperelastic, Viscoelasticity, Viscoplasticity, Saturation damage, Glassy polymers

ABSTRACT

The aim of this work is to develop an efficient large-strain hyperelastic constitutive model for amorphous polymers in the glassy state. These materials exhibit a complex rate- and pressure-sensible behavior in both elastic and plastic regimes. After an initial linear elastic region, a nonlinear stage continues until reaching a peak stress, which is followed by a softening stage. At large strains, when the softening is saturated, a re-hardening stage is reached. The viscoelastic effect is captured using the generalized Maxwell model. The viscoplastic effect is considered using a Perzyna-type flow rule incorporating a pressure sensitive yield surface and a non-associated flow potential. This yield surface is extended from the Drucker-Prager one. The saturated softening phenomenon is modeled using an isotropic numerical damage variable progressed by a saturated softening law. With the introduction of the damage parameter, a non-local implicit gradient damage model is used to avoid the loss of the solution uniqueness. Through experimental comparisons, it is shown that the proposed model has the ability to model the complex mechanical responses of amorphous glassy polymers.

1 INTRODUCTION

The amorphous polymers in the glassy state are often used as matrix materials in polymer reinforced composites, which appear in a large range of applications in the aerospace and automotive industries. In their glassy state, these materials exhibit rate-, time-, pressure-, and temperature-dependent response, see [1] for more details in case of the RTM6 epoxy resin. Moreover, different stages can be identified in the stress-strain curves from experiments [2]. After an initial linear elastic region, a nonlinear stage continues until reaching a peak stress, which is followed by a softening stage. At large strains, when the softening is saturated, a re-hardening stage is reached. The rate effects are significant even at low strain level. As a consequence, a constitutive model incorporating the viscoelastic, viscoplastic, and damage ingredients is necessary to capture the whole range of the polymer response.

Using a hyperelastic formulation, the constitutive model is based on an elastic potential, from which the first Piola-Kirchhoff can be obtained by derivation with respect to its work conjugated measure, which is the deformation gradient. The viscoelastic effect is modeled using the generalized

Maxwell model constructed from the corotational Kirchhoff stress and the elastic logarithmic strain. The viscoplastic effect is based on a Perzyna-based flow rule [3] incorporating a pressure-sensitive yield function and a non-associated flow potential. This yield surface is extended from the Drucker-Prager one. A quadratic flow potential is used to correctly capture the volumetric deformation during the plastic process with a constant plastic Poisson ratio [4]. The saturated softening phenomenon is introduced to the constitutive law through an isotropic damage variable, which is saturated by a limit value. The rehardening stage is naturally obtained after the damage saturation because of the kinematic and isotropic hardening phenomena, which are still developing. With the introduction of the damage, the non-local implicit gradient damage model [5] is used to avoid the loss of the solution uniqueness. With these ingredients, the proposed model is shown to capture the full range of the mechanical behavior of the amorphous glassy polymers at various strain rates, as compared to the experiments.

2 CONSTITUTIVE MODEL

Following the standard multiplicative decomposition in elastoplastic materials at finite strains, the deformation gradient tensor \mathbf{F} is decomposed into a recoverable (viscoelastic) component and an irrecoverable (viscoplastic) component, following

$$\mathbf{F} = \mathbf{F}^{ve} \cdot \mathbf{F}^{vp}, \quad (1)$$

where \mathbf{F}^{ve} and \mathbf{F}^{vp} are the viscoelastic and viscoplastic tensors, respectively. Based on the continuum damage mechanics, the damage represents the relation between the stresses in the apparent body and in its undamaged representation [6]. This relation can be written as

$$\hat{\mathbf{P}} = \frac{\mathbf{P}}{1-D}, \quad (2)$$

where \mathbf{P} is the first Piola-Kirchhoff stress in the apparent body, $\hat{\mathbf{P}}$ is the effective (undamaged) counterpart in the undamaged representation, and $0 \leq D < 1$ is the numerical damage variable used to represent the softening response. In this work, the saturation damage phenomenon is considered with a limit value $D_\infty < 1$.

The hyperelastic formulation is based on the existence of an elastic potential Ψ . The stress measures are derived from this potential function by the relation

$$\delta\Psi = \hat{\mathbf{P}} : \delta\mathbf{F} = \hat{\mathbf{k}} : (\delta\mathbf{F} \cdot \mathbf{F}^{-1}) = \hat{\boldsymbol{\tau}} : \delta\mathbf{E}^{ve}, \quad (3)$$

where $\hat{\mathbf{P}}$ is the effective first Piola-Kirchhoff stress, where $\hat{\mathbf{k}}$ is the effective Kirchhoff stress and where $\hat{\boldsymbol{\tau}}$ is the effective corotational Kirchhoff stress, which is the stress measure conjugated to the viscoelastic logarithmic strain $\mathbf{E}^{ve} = \ln \sqrt{\mathbf{C}^{ve}}$ with the viscoelastic right Cauchy strain tensor $\mathbf{C}^{ve} = \mathbf{F}^{veT} \cdot \mathbf{F}^{ve}$. The effective Cauchy stress can be computed from the relation $\hat{\boldsymbol{\sigma}} = J^{-1} \hat{\mathbf{P}} \cdot \mathbf{F}^T = J^{-1} \hat{\mathbf{k}}$, with $J = \det \mathbf{F}$.

2.1 Viscoelastic part

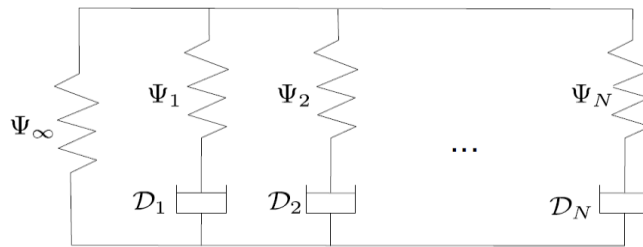


Figure 1: Springs/dashpots network of the generalized viscoelastic Maxwell model.

The viscoelastic behavior is modeled using the generalized Maxwell model. This model contains $N+1$ elastic springs and N dashpots as shown in Figure 1. The total elastic potential is given by

$$\Psi = \Psi_{\infty} + \sum_{i=1}^N \Psi_i - D_i, \quad (4)$$

where Ψ_i with $i = \infty, 1, \dots, N$ are the elastic potentials acting on the springs and where D_i with $i = 1, \dots, N$ are the dissipating functions acting on the dashpots. In each spring, the elastic potential is defined as

$$\Psi_i = \frac{K_i}{2} \ln^2 J^{ve} + G_i \text{dev} \mathbf{E}^{ve} : \text{dev} \mathbf{E}^{ve} \text{ with } i = \infty, 1, \dots, N, \quad (5)$$

where K_i and G_i are respectively the bulk and shear moduli and where $J^{ve} = \det \mathbf{F}^{ve} > 0$ is the viscoelastic Jacobian. From the elastic potential given by Eq. (5), the related effective corotational Kirchhoff stress is derived as

$$\begin{aligned} \hat{\boldsymbol{\tau}}_i &= \frac{\partial \Psi_i}{\partial \mathbf{E}^{ve}} - \frac{\partial D_i}{\partial \mathbf{E}^{ve}} = K_i \text{tr}(\mathbf{E}^{ve}) \mathbf{I} + 2G_i \text{dev} \mathbf{E}^{ve} - \mathbf{q}_i \\ &\quad \text{with } i = 1, \dots, N, \quad (6) \\ \hat{\boldsymbol{\tau}}_{\infty} &= \frac{\partial \Psi_{\infty}}{\partial \mathbf{E}^{ve}} - \frac{\partial D_{\infty}}{\partial \mathbf{E}^{ve}} = K_{\infty} \text{tr}(\mathbf{E}^{ve}) \mathbf{I} + 2G_{\infty} \text{dev} \mathbf{E}^{ve} \end{aligned}$$

where \mathbf{q}_i is the internal variables governing the viscoelastic behavior. The viscoelastic effect is added through the internal variables by a retardation action. For the spring/dashpot branch i , the viscoelastic equations are given as follows

$$\text{dev}(\dot{\mathbf{q}}_i) = \frac{\text{dev}(\hat{\boldsymbol{\tau}}_i)}{g_i}, \quad \text{tr}(\dot{\mathbf{q}}_i) = \frac{\text{tr}(\hat{\boldsymbol{\tau}}_i)}{k_i}, \quad i = 1, \dots, N, \quad (7)$$

where g_i and k_i are the characteristic retardation times for the deviatoric and volumetric parts, respectively. Equations (6) and (7) lead to the solution of the effective corotational Kirchhoff stress $\hat{\boldsymbol{\tau}}_i$ on each spring/dashpot branch. The total effective corotational Kirchhoff stress $\hat{\boldsymbol{\tau}}$ is computed from the convolution form in time as

$$\hat{\boldsymbol{\tau}}(t) = \hat{\boldsymbol{\tau}}_{\infty} + \sum_{i=1}^N \hat{\boldsymbol{\tau}}_i = \int_{-\infty}^t \mathbf{C}^{ve}(t-s) : \frac{\partial}{\partial s} \mathbf{E}^{ve}(s) ds, \quad (8)$$

where the fourth order Hook tensor is given by

$$\begin{aligned} \mathbf{C}_{ijkl}^{ve}(t) &= K(t) \delta_{ij} \delta_{kl} + G(t) \left(\delta_{ik} \delta_{jl} + \delta_{il} \delta_{jk} - \frac{2}{3} \delta_{ij} \delta_{kl} \right), \\ K(t) &= K_{\infty} + \sum_{i=1}^N K_i \exp\left(-\frac{t}{k_i}\right), \\ G(t) &= G_{\infty} + \sum_{i=1}^N G_i \exp\left(-\frac{t}{g_i}\right). \end{aligned} \quad (9)$$

Finally, the effective first Piola-Kirchhoff stress is estimated using Equations (3) and (8) as

$$\hat{\mathbf{P}} = \mathbf{F}^{ve} \cdot \left(\hat{\boldsymbol{\tau}} : \frac{\partial \ln \mathbf{C}^{ve}}{\partial \mathbf{C}^{ve}} \right) \cdot \mathbf{F}^{vp-T}. \quad (10)$$

2.2 Viscoplastic part

In order to model the viscoplastic behavior, a Perzyna-type viscoplastic flow rule [3] is used. The viscoplastic deformation evolution can be estimated with the following relation

$$\mathbf{D}^p = \frac{1}{\eta} \langle F \rangle_p^{\frac{1}{p}} \frac{\partial P}{\partial \hat{\boldsymbol{\tau}}}, \quad \langle F \rangle = \begin{cases} F & \text{if } F \geq 0 \\ 0 & \text{if } F < 0 \end{cases}, \quad (11)$$

where \mathbf{D}^p is the viscoplastic strain rate, where F is the yield function, where P is the flow potential, where η is the viscosity, and where p is the rate sensitivity exponent. In the viscoplastic range, a new yield condition can be defined as

$$\bar{F} = F - (\eta\lambda)^p \leq 0, \quad \text{with } \lambda = \frac{1}{\eta} \langle F \rangle_p^{\frac{1}{p}}, \quad (12)$$

which is completed by the Kuhn-Tucker condition,

$$\bar{F} \leq 0 \quad \lambda \geq 0 \quad \lambda \bar{F} = 0. \quad (13)$$

To model the pressure sensitive effect in amorphous glassy polymers, a generalized version of the classical Drucker-Prager is considered with a power-enhanced octahedral term of exponent α , such as

$$F = \left(\frac{\chi_{eq}}{\sigma_c} \right)^\alpha - \frac{m^\alpha - 1}{m+1} \frac{\text{tr}(\boldsymbol{\chi})}{\sigma_c} - \frac{m^\alpha + m}{m+1}, \quad \text{tr}(\boldsymbol{\chi}) = \chi_{ii}, \quad \chi_{eq} = \sqrt{\frac{3}{2} \text{dev} \boldsymbol{\chi} : \text{dev} \boldsymbol{\chi}}, \quad m = \frac{\sigma_t}{\sigma_c}. \quad (14)$$

In Eq. (14), $\boldsymbol{\chi} = \hat{\boldsymbol{\tau}} - \mathbf{b}$ is the combined stress tensor, $\hat{\boldsymbol{\tau}}$ is the effective corotational Kirchhoff stress tensor expressed in Eq. (8), \mathbf{b} is the back-stress tensor, which is used to capture the kinematic hardening effect, σ_c and σ_t are the isotropic compression and tensile yield stresses, respectively, and m is the traction/compression yielding anisotropy. The arbitrary value of the exponent α can be used leading to a new class of yield surface, so-called power yield surfaces. If $\alpha = 1$, the classical Drucker-Prager one is recovered; if $\alpha = 2$, the paraboloidal one is obtained. Both of them can be used for amorphous glassy polymers [4].

A non-associated flow rule is assumed in this work. The flow potential in Eq. (11) is specified with a quadratic function of the corotational Kirchhoff stress as

$$P = \chi_{eq}^2 + \beta \left[\frac{\text{tr}(\boldsymbol{\chi})}{3} \right]^2, \quad (15)$$

where β is the flow parameter. Using this non-associated flow, the constitutive model has the ability to capture the volumetric plastic deformation with a constant plastic Poisson ratio, which is directly related to the flow parameter through the relation [4]

$$\nu_p = \frac{9 - 2\beta}{18 + 2\beta}. \quad (16)$$

The equivalent plastic deformation rate is defined from the viscoplastic strain rate tensor in Eq. (11) by the following relation [4]

$$\dot{\gamma} = \frac{1}{\sqrt{1 + 2\nu_p^2}} \sqrt{\mathbf{D}^{vp} : \mathbf{D}^{vp}}. \quad (17)$$

2.3 Saturated damage evolution

Using the coupled damage concept of Eq. (2), the remaining part is to provide the evolution of the isotropic numerical damage parameter. This work uses the non-local accumulated plastic strain $\bar{\gamma}$ to compute the damage evolution, as

$$D = D(\mathbf{F}, \bar{\gamma}), \quad (18)$$

with the assumption that the damage depends only on the strain state and on the non-local variable. In this non-local enhanced model, the non-local accumulated plastic strain is computed from the implicit formulation [5]

$$\bar{\gamma} - c\Delta\bar{\gamma} = \gamma, \quad (19)$$

where c is the square of the characteristic non-local length. The relation (20) is completed by the natural boundary condition

$$\nabla\bar{\gamma} \cdot \mathbf{n} = 0. \quad (20)$$

The evolution of damage follows a saturation law

$$\dot{D} = \begin{cases} 0 & \text{if } \bar{\gamma} < \gamma_c \\ h\bar{\gamma}^s (D_\infty - D)\dot{\bar{\gamma}} & \text{if } \bar{\gamma} \geq \gamma_c \end{cases}, \quad (21)$$

where D_∞ is the saturation damage value, h is the softening slope, s is the softening exponent and γ_c is the plastic threshold for the damage evolution.

3 COMPARISON WITH EXPERIMENTS

The numerical compression and creep predictions of epoxy resins at the room temperature (23°C) using the current viscoelastic-viscoplastic-damage constitutive model are illustrated in Figure 2, where they are compared to the experimental curves reported in [2]. The obtained results are in good agreement with the experiments showing the ability of the proposed model for predicting the behavior of amorphous glassy polymers.

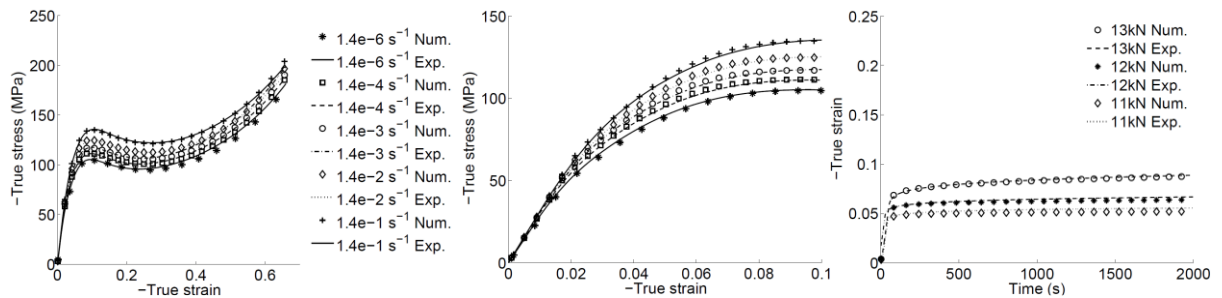


Figure 2: Model predictions compared to the experimental data [2] at room temperature: uniaxial compression results at various strain rates in the full strain range (left image), zoom at small strain levels (middle image); creep test results (right image).

4 CONCLUSIONS

The developed model can correctly capture the overall response of amorphous glassy polymers with the epoxy resins as a specific case through a couple viscoelastic-viscoplastic-damage constitutive model. The implicit non-local plastic model is employed to avoid the loss of uniqueness. In the near future, an appropriate pressure-dependent failure criterion is incorporated. The constitutive model will be applied to the polymer resins of composites, so that the multi-scale fracture of composites will be

studied using the Discontinuous Galerkin/Cohesive Zone Method (DG/CZM) as proposed in [7].

ACKNOWLEDGEMENTS

The author gratefully acknowledge the financial support from F. R. S. – F. N. R. S. under the project number PDR T.1015.14.

REFERENCES

- [1] F. Lani, X. Morelle, C. Bailly, and T. Pardoën, “Characterization and modeling of the strain-rate, temperature and pressure dependence of the deformation of a highly crosslinked aerospace grade epoxy resin,” in *20th International Conference on Composite Materials ICCM20*, 2015.
- [2] X. Morelle, F. Lani, M. Melchior, S. Andre, C. Bailly, and T. Pardoën, “The elasto-viscoplasticity and fracture behavior of the RTM6 structural epoxy and impact on the response of woven composites,” in *15th European Conference on Composite Materials*, 2012.
- [3] P. Perzyna, *Thermodynamic theory of viscoplasticity*, vol. 11. Elsevier, 1971.
- [4] A. R. Melro, P. P. Camanho, F. M. Andrade Pires, and S. T. Pinho, “Micromechanical analysis of polymer composites reinforced by unidirectional fibres: Part I – Constitutive modelling,” *International Journal of Solids and Structures*, vol. 50, no. 11–12, pp. 1897–1905, Jun. 2013.
- [5] R. H. J. Peerlings, R. De Borst, W. a M. Brekelmans, and J. H. P. De Vree, “Gradient enhanced damage for quasi-brittle materials,” *International Journal for Numerical Methods in Engineering*, vol. 39, no. 19, pp. 3391–3403, 1996.
- [6] J. Lemaitre, “Coupled elasto-plasticity and damage constitutive equations,” *Computer Methods in Applied Mechanics and Engineering*, vol. 51, no. 1–3, pp. 31–49, Sep. 1985.
- [7] L. Wu, D. Tjahjanto, G. Becker, A. Makradi, A. Jérusalem, and L. Noels, “A micro–meso-model of intra-laminar fracture in fiber-reinforced composites based on a discontinuous Galerkin/cohesive zone method,” *Engineering Fracture Mechanics*, vol. 104, pp. 162–183, May 2013.